

Comparative Imagery Analysis of Non-Metric Cameras from Unmanned Aerial Survey Aircraft

Jason Poser

Department of Resource Analysis, Saint Mary's University of Minnesota, Winona, Minnesota 55987

Keywords: GIS, UAS, UAV, Photogrammetry, DTM, GCP, Non-Metric, GSD, Orthomosaics

Abstract

Unmanned aerial survey imagery from non-metric cameras was analyzed for suitability, stability, and resolution within a geographic information system. A powered parachute aircraft was designed for the research and used to obtain imagery using two cameras. The research implemented three commercial photogrammetry applications to assess and isolate any application specific nuances that may affect the resulting datasets. Using Esri's ArcMap, a comparative analysis of the resulting orthomosaics and digital terrain models was conducted. The findings of the research indicate that quality datasets obtained using the methods described are plausible and realistic. Expectations of spatial accuracy and terrain resolution were met.

Introduction

Aerial imaging started more than 150 years ago. According to the Professional Aerial Photographers Association (2012), aerial photography was first practiced by French photographer and balloonist Gaspard- Félix Tournachon ("Nadar"). Unfortunately those early photographs no longer survive. The oldest aerial photograph known to exist is James Wallace Black's image of Boston in 1860.

It was not until World War I that aerial photography made by aerial observers replaced drawings and sketches of the battlefields. By the end of the war aerial photographs were recording the entire front twice daily. At the end of the war aerial cameras first transitioned to non-military purposes when in 1921 Sherman Fairchild produced overlapping photographs that made a map of Manhattan Island (Professional Aerial Photographers Association, 2012). This

aerial map was a commercial success and used throughout New York City's administrative agencies and businesses. With other cities following, aerial surveys proved to be faster and less expensive than traditional ground surveys.

Today, 91 years after Sherman Fairchild made his Manhattan Island map, with the advent and rapid adoption of web-based consumer mapping products such as Google Earth and Bing maps, the demand and use for aerial imaging has become common in consumer navigation and mobile web-based location information services. Aerial imagery has become a common spatial background from which other feature datasets are created. The demand for ever increasing accuracy and resolution for a lower cost and faster delivery is the primary motivation for this research. Advancements in camera technology and the reduction in camera costs have made it possible to obtain low-cost ultrahigh resolution spatially accurate

imagery in a static environment.

In addition to advancements in camera technology, advancements in flight technology have also occurred including the rise of the unmanned aerial vehicle (UAV) industry. Rapid development of the UAV industry can be largely credited to military research and development during the last decade. Companies such as Boeing, Lockheed Martin, BAE, and Northrop Grumman are changing the way data are collected in theatres of conflict across the globe and are influencing new innovation commercially (Abramson, 2012).

The acceptance of civil market UAV usage is rapidly approaching and Congress, the FAA, and the nation are questioning the role and scope in which civil UAV use in commercial airspace will be permitted, with safety and privacy being the two highest concerns. This paper will not focus on social and legal implications of UAV use in the United State's airspace as these are serious and complicated issues that need to be considered before unmanned aircraft are widely adopted.

The purpose of this paper is to provide a methodology to validate imagery derived from unmanned aerial vehicles for use in civil geospatial projects. The fundamental question is whether or not the combination of digital aerial image sensors coupled with unmanned aerial vehicles can produce reliable, consistent, commercially comparable datasets that represent as good or better resolution for use in geographic information system (GIS) centric mapping as presently exists. For UAV-based aerial imagery to be considered useful for this project, it is important that UAV-derived imagery be of a calculable quality compared to that of traditional aerial imagery products. The direction of this research is to illustrate a GIS approach for

the analysis of UAV-derived spatially accurate imagery.

An attempt was made in this research to determine appreciable imagery differences between two different sensors on board a UAV aircraft. Current commercial UAV systems are fully capable of supporting a wide range of digital sensors; however most of the existing imaging systems currently used are largely cost-prohibitive for the civil market and small budget programs. However, smaller boutique hobbyist grade UAV systems are rapidly entering the market with increased accuracy and lower cost making unmanned aerial surveys more feasible. These systems are largely limited to supporting small consumer-grade non-metric cameras typically weighing less than 600g. This research specifically evaluates the effectiveness of non-metric cameras on board UAV aircraft for use in aerial imaging.

Photogrammetry Software

Traditional aerial photogrammetry workflows are developed to work in conjunction with imagery captured from precisely controlled piloted aircraft. The unique nature and variability of unmanned aerial vehicle surveys may present challenges for existing aerial photogrammetry software systems in how they process the datasets. One component of this research is to analyze and attempt to isolate the relationship between the inherent raw image accuracy and processed image accuracy.

Non-metric Camera Geometric Stability

Imaging system performance depends on several variables. In addition to the camera's sensor size, its lens system, aperture, ISO capability, and frame rate

each contribute a unique set of performance factors to the overall system design. Metric and non-metric is one way of classifying cameras used for obtaining aerial imagery. Metric cameras are constructed following strict criteria related to internal camera dimensions. These cameras are certified to perform consistently from image capture to image capture without variation in image distortion. Non-metric cameras such as most consumer-grade cameras are not designed to meet these rigorous standards. Often non-metric cameras have variable zoom focus lenses which add yet another level of uncertainty to the camera's stability over time.

A second component of the research was to explore whether current non-metric cameras provide for reasonably consistent results in terms of geometric stability for use in aerial survey. Can non-metric point and shoot cameras of good to excellent quality provide the geometric stability that is traditionally required by commercial aerial photogrammetry software packages? Furthermore, it is expected that measurable differences in the camera calibration will occur over time being that the lens system auto retracts during each power cycle whereas fixed focal length systems typically retain their geometric stability regardless of the power cycle. Previous data suggests non-metric cameras can perform well in terms of photogrammetric stability (Stahlke, 2011). For this study, camera calibration results before and after flight were used to explore this question as well as the performance of the photogrammetry software with the input parameters from the camera calibration.

Methods

Vehicle Platform

Three UAV aircraft were designed and fabricated for this research, while only one aircraft was used for actual data collection (Figures 1 and 2). In terms of time and resources, the process of designing, fabricating, and testing was by far the most laborious component of this project. To that degree, a firm understanding of how the research aircraft impacts the imagery needed to be explored and tested.



Figure 1. Powered parachute UAVs designed and fabricated as part of the research.



Figure 2. Powered parachute UAV aircraft designed and fabricated as part of the research.

Three distinct platforms were considered for the research: fixed-wing aircraft, multi-rotor helicopter, and a powered parachute. Ultimately, the aircraft design series that was chosen was designed around powered parachutes. The criteria needed for the platforms were:

1. Safety: The aircraft needed to be able to prevent harm to the general public and/or damage to the calibrated cameras used in the research.
2. Relatively slow airspeed to help minimize motion image blur.
3. Large configurable payload capability to host several sensor configurations depending on the data that needs to be collected.

The most suitable aircraft in terms of technical abilities was a multi-rotor helicopter. Multi-rotor helicopters offer precise flight control with vertical lift and landing capabilities that are ideal for small area studies. The defining drawback to these systems is the safety. The multi-rotor helicopters use multiple precisely timed motors, multiple motor controllers, and multiple propellers to maintain stable flight. Should any of these components fail, the helicopter's stability deteriorates at an alarming rate and commonly results in an uncontrolled free fall crash.

Powered parachutes were the most suitable platform when the research commenced. Powered parachutes fly relatively slow using a ram airfoil parachute. Lift is generated by the parachute when the baffles of the parachute are inflated; the inflated parachute creates a wing surface like that of a typical aircraft. In the unlikely event of total electrical failure resulting in the loss of navigation and propulsion, a powered parachute would pose the least risk to injury and property of the general public.

Image Sensors

To test the question of geometric stability of variable focus point-and-shoot consumer cameras, two cameras were used

for this research: Canon G10 and Canon S60. The Canon G10 has a maximum imaging resolution of 4416 x 3312 pixels (14.62 megapixels) and a 6.1 mm lens (Canon, 2012a). The sensor is a 1/1.7-inch type Charge Coupled Device (CCD) (Canon, 2012a). The Canon S60 has a maximum imaging resolution of 2592 x 1944 pixels (5.0 megapixels) and a 5.8 mm lens (Canon, 2012b). The sensor is a 1/1.8 inch CCD (Canon, 2012b).

Camera Calibration

The first stage of the research was to establish a camera control model that served as a baseline for the geometric stability of the cameras throughout the research. If questions arose about lens and sensor stability, the initial camera calibration could be compared for any potential errors.

Three camera calibration objects were used in order to assess the consistency in the results over time and between calibration objects. Two of the three objects are stationed at the United States Geological Survey (USGS) Earth Resources Observation Systems facility (EROS) in Sioux Falls, South Dakota. Each camera was calibrated at the USGS photogrammetry facility to establish initial calibrations. The primary calibration object was the Pictometry® designed calibration cage from which all other calibrations in this research were measured and compared (Figure 3).

The second calibration object was the prototype calibration box designed by Don Moe, Principal Photogrammetrist at the USGS EROS facility. Its purpose is to test short focal length cameras for photogrammetric stability and accuracy.

The third calibration object, the field box, was developed for this research



Figure 3. The USGS aerial camera photogrammetry calibration cage.

as the workhorse of the calibration workflow process (Figure 4). It was designed based upon the specifications of the USGS prototype close range calibration box. The nature of the research dictated that each camera could be calibrated in the field if needed. For this reason the field calibration box was ruggedized, constructed with aluminium reinforced 1" treated cabinet grade plywood in order to maintain its relative geometry from project site to project site. The field box was designed to sit on the ground to allow the calibration process to rotate around the object unobstructed. At 2'square and 10.5" deep, it supported 53 two-millimeter Photometrix AutoCal targets to facilitate near automatic calibration processing.

The color, finish, and interior texture of the field box were carefully chosen. The gray interior tint was selected to contrast between the Photometrix AutoCal targets and the background while minimizing potential reflective glare. Initial paint finish tests were tested for durability. Flat gray paint was shown to be ideal for imaging by reducing glare; however, flat finishes are susceptible to scratching and marring when touched. Ultimately a semi-gloss finish was used to maintain a consistent image surface over time. Special care was taken to reduce the

textures within the interior. A smooth surface, free of bumps and dents reduced possible artifacts and noise on the images.

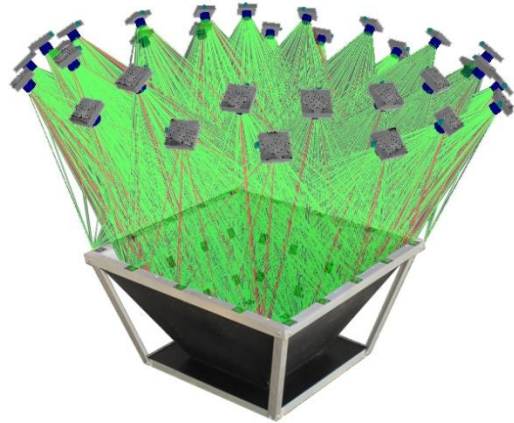


Figure 4. Composite representation of the actual calibration Field Box against an actual Australis software calibration.

The software used for the calibration process was Australis by Photometrix. To reduce error, the research employed the same calibration software as the USGS. If anomalies arose, the datasets could be evaluated on isolated systems to rule out errors.

Photogrammetric Triangulation

In order to solve for photogrammetric image position within the aerial triangulation software, the position of the sensor relative to the ground is needed. Often high-end hardware and software capture systems employ inertial measurement units (IMUs) in combination with global positioning systems (GPS) to determine the sensor's orientation at the time of capture. The size and cost of these high-end systems generally excludes their use within smaller UAV systems. Inertial measurement units are thus beyond the scope of this research and is the reason that the space resection method was used to define the exterior orientation in lieu of

the IMU systems described above.

Space resection using collinearity condition is a photogrammetric technique that is used to establish the exterior camera orientation associated with one or multiple images based on at least three known ground coordinates per image (ERDAS, 2010). These known ground coordinates are commonly referred to as ground control points. A ground control point (GCP) is a specific point/pixel for which a ground coordinate is known. They are referenced in a three-dimensional coordinate system (X, Y and Z) in combination with a projection and are typically expressed in feet or meters (ERDAS, 2010).

The exterior orientation directly defines the angular orientation of an image. The elements of exterior orientation are variables of the image position at moment of capture (ERDAS, 2010). The positional orientations include X_o , Y_o , and Z_o . They establish the position of the perspective center (O) with regards to the coordinate system of the ground, where Z_o is commonly known as the height of the camera above sea level defined by a datum. The three rotational angles determined are omega, phi, kappa (the rotations about the three axis). These six camera orientation measures (X_o , Y_o , Z_o , omega, phi, kappa) are combined with internal camera measurements from the camera calibration report to determine the internal sensor's orientation at the time of image capture (ERDAS, 2010).

Study Site

A 100' x 100' study area was established on a gently sloped low-vegetation hayfield (Figure 5). The study area consisted of eight ground control points forming the perimeter of the 100' x 100' study area and 17 randomly spaced ground control points

for the establishment of the interior space (Appendix A). An initial survey to establish ground control points used Real-Time Kinetic (RTK) GPS. Wooden survey stakes in conjunction with plastic flags were used to mark out the ground control point positions. Horizontal X, Y and Z elevation were captured.



Figure 5. Survey area.

Twenty-five 15" square black and white aerial marking targets were centered on the wooden survey stakes (Figure 6). After the aerial targets were in place, a total station survey was performed as a measure of control against the RTK GPS survey.



Figure 6. Aerial target 15"x15"sq.

The total station survey used two of the RTK GPS points as reference points; therefore, the total station survey was not used to verify absolute elevation, but rather to verify that the measurements between GCPs were within acceptable deviation. The average difference in control point elevation between the total station and RTK GPS was 0.24 inches with a standard deviation of 0.64 inches.

To further verify that the survey results were a reasonable method for obtaining ground control point coordinates, the elevation values were compared to light detection and ranging (LIDAR) data representing bare earth with a 3.90' resolution. The dataset was acquired from Ayres Associates. The RTK GPS values were compared to elevation values derived from a digital terrain model interpolated from LIDAR point data. The average difference between the RTK GPS elevation values and the LIDAR elevation values was 2.05 inches, with a standard deviation of 0.78 inches. This difference was deemed reasonable considering the LIDAR surface was derived from points spaced approximately 4 feet apart. The LIDAR interpolation process could have introduced error at locations on the surface in between the LIDAR points. Based on these results, it was concluded that the RTK GPS control point measurements were reasonable for use in the orthorectification process of the aerial imagery.

Data Capture

The criteria for research flights were carefully designed to maximize commonality between the different flights and minimize environmental variability that could skew the overall data collected. The criteria were:

1. Wind conditions could not exceed 4mph for the day.
2. Overcast conditions were required to minimize shadow casting and direction issues.

Over the course of one day, four flights were conducted. Each camera was flown twice to ensure enough coverage was obtained over the research study area. From the four flights, two flights were selected for use in the research.

Image Processing

Photogrammetry has been defined by the American Society for Photogrammetry and Remote Sensing as “the art, science, and technology of obtaining reliable information about physical objects and the environment through processes of recording, measuring and interpreting photographic images and patterns of recorded radiant electromagnetic energy and other phenomena (ASPRS, 2009).” The photogrammetric workflow has remained relatively unchanged since the advent of digital photogrammetry. This consists of projects created where the operator defines the coordinate system and ancillary information such as flying height and sensor type. Camera information is then added to the workflow. Traditionally aerial imaging camera information is stored in an external camera file which contains information regarding the camera’s focal length, principal point offsets, and radial lens distortions that are generated from the camera calibration report. Space resection is performed and the X, Y, Z, omega, phi, kappa orientation parameters are combined with the interior orientation parameters to calculate the exterior orientation.

Aerial triangulation orients the images in relation to each other and also to

the ground coordinate system. This translates to establish that every pixel refers to a coordinate. Ground control points are used both in workflows where the exterior orientations are known and unknown. In projects such as this one, where the exterior orientation is unknown, ground control points are used to reverse triangulate for the camera's interior orientation using a process known as exterior camera orientation. The establishment of an initial approximation of the orientation parameters (i.e., rough orientation) is then processed further using a semi-automatic process in which additional tie points are identified and matched throughout corresponding images to strengthen the matching accuracy. The final bundle block adjustment is performed and refined by removing inaccurate points until the solution is within acceptable error tolerances.

Digital terrain generation is performed automatically and the terrain generation algorithms typically match terrain points on one or two images. Ground control points and other data can often be supplied to help guide the correlation process. Terrain editing follows digital terrain generation. This automated process is to remove and perform cleanup of extraneous points. Orthomosaics are typically the final product derived from the photogrammetric workflow.

Three distinctly different photogrammetry applications were chosen to process the datasets in a side-by-side comparison: ERDAS LPS, Agisoft PhotoScan, and Pix4D (described in more detail below). The objective of using three photogrammetry applications was to observe the range of results produced through data processing.

While the underlying fundamentals of photogrammetry similarly

span across the applications used in this study to process the research data, it is suspected that design of the software, and for what industry it was made to serve, can greatly dictate the achievable results from a standard set of inputs and user defaults. The defining commonality between the three chosen applications was the use of space resection and ground control points as input. Ground control points were added into the routines of each application during the processing of the datasets. Furthermore, the coordinate system and projection of the ground control point inputs were identical, forcing each application to utilize the same three-dimensional space when processing the data.

Orthorectification

Aerial imagery is a representation of irregular surfaces and texture. Seemingly flat images are actually distorted due to the physical curvature of terrain being imaged and the imaging sensor used. Rectification is the process of geometrically correcting the image to be planar so it matches the corresponding images when in a flat orientation (ERDAS, 2010).

While not necessary with featureless flat areas of study, orthorectification is a more robust form of rectification that implements digital terrain models and uses collinearity equations and ground control points to better compensate for areas where dramatic changes in elevation reside (ERDAS, 2010). For the purpose of this research orthorectification is used to best represent the data and analysis.

Software Descriptions

ERDAS LPS is one of the leading photogrammetry workhorse software

programs available today. Owned by Intergraph Corporation, ERDAS LPS is tailored for remote-sensing professionals and large commercial and governmental agencies. Capable of processing satellite, LIDAR, aerial imaging, and in some cases terrestrial datasets, it offers the greatest range and capability for processing remotely sensed data. ERDAS LPS offers the widest range of end-user specified options of the applications tested, ranging from terrain elevation model outputs including accuracy, radiometric quality, ground sample distance, output projections and output file format.

Agisoft PhotoScan is a standalone photogrammetric application that follows a linear, project-based workflow. Raw data added to the workflow requires a camera model be assigned to each image. This model consists of the focal length, principal point, and lens distortion coefficients. This particular application automatically applies the Brown model and estimates the calibration coefficients during processing (Agisoft, 2012). Should the automatic calibration fail, calibration parameters are then entered into Agisoft PhotoScan to achieve optimal reconstruction results. Automatic tie point production, based on detection points of interest and matching, is first processed. Geometric accuracy improves with the addition of GCPs being entered into the project. Next, aerial triangulation is run, Dense Surface Reconstruction is processed, and the resulting digital terrain model (DTM) is created (Agisoft, 2012). With the digital terrain model, Agisoft PhotoScan uses a triangulated irregular network (TIN) surface to correct for terrain displacement and exterior orientations for georeferencing and creation of the orthoimage (Agisoft, 2012).

Pix4D is both an online service and

stand-alone application specifically designed for unmanned aerial vehicle survey imagery datasets. For this research the automated online service was utilized. First Pix4D computes the true locations and parameters of the original images through Automatic Aerial Triangulation (AAT) and Bundle Block Adjustment (BBA). Based on the cloud of 3D points retrieved during the AAT and the BBA, a digital surface model is generated by connecting these points. The number of 3D points is then further increased to reach up to pixel level point clouds. The orthomosaic is finally created by projecting and blending the original images with the digital surface model.

Processing Outputs

The two flights selected for use in the research represented one flight with each image sensor (Canon G10 and Canon S60). Each application produced one orthomosaic and one digital terrain model per set of imagery. The complete catalog of results consisted of six orthomosaics and six digital terrain models representing the complete range of photogrammetry derived datasets:

1. G10 processed with Agisoft PhotoScan
2. G10 processed with ERDAS LPS
3. G10 processed with Pix4D
4. S60 processed with Agisoft PhotoScan
5. S60 processed with ERDAS LPS
6. S60 processed with Pix4D

Functional Measures of Image Quality

Within Esri's ArcMap software a systematic approach was devised to assess the final datasets in order to characterize the accuracy and overall value of UAV

imagery for use in civil GIS applications. Three methods were used to: 1) explore positional accuracy of the orthomosaics, 2) explore performance in image classification, and 3) explore the difference in surface area between the digital terrain models.

To determine the spatial accuracy of the resulting orthomosaics, the RTK survey points were compared to the targets in the photos. Each orthomosaic was added to ArcMap and a point dataset was digitized marking the visual centers of the targets in the photos. The X, Y, and Z coordinates of these digitized points were calculated using built-in ArcMap functionality. The coordinates were then exported to Microsoft Excel and compared to the RTK survey coordinates.

To determine image classification performance, the white areas of the targets were classified using the red, green, blue (RGB) values of the cells in the orthomosaics and the Raster Calculator tool in ArcMap. The resulting white areas were measured and compared to the known total white area of all targets in the image.

The surface area analysis was implemented to accurately calculate the changes across the range of digital terrain models using Esri's Surface Volume (3D Analyst) tool within ArcMap. According to Esri (2012), the ArcMap 3D Surface Volume tool "calculates the area and volume of a raster, triangulated irregular network (TIN), or terrain dataset surface above or below a given reference plane."

Ground Sample Distance

Ground sample distance (GSD) (commonly referred to as spatial resolution) is a typical derivative of the image processing output and is often referenced as a general form of image

measurement. The GSD is a description of how large an area on the ground each pixel represents in an image. It has been defined as the horizontal distance in ground space between the centers of two adjacent pixels in an image (BAE Systems, 2010). In the simplest context, GSD is calculated by:

$$\text{GSD} = (\text{pixel element size}) \times H_g / f$$

(Matthews, 2008)

Where pixel element size is the size of each pixel in the CCD array and is calculated by taking the physical width of the sensor divided by the width of the sensor in pixels (Matthews, 2008).

Where H_g is the average flying height above the ground.

Where f is the focal length of the lens.

What this represents is a linear relationship where a change in the values H_g or f will result in changes in image distances by the same factor (Small-Format Aerial Photography, 2010). The output of the aforementioned equation represents the ideal best achievable GSD in a mathematically perfect situation and thus is theoretical. Aerial photographs will deviate from this idealized situation mainly in three ways (Aber, Marzoff, and Ries, 2010):

1. The elevation of the camera relative to the ground varies within an image due to differences in terrain elevation within the image footprint.
2. The sensor and lens being off nadir at the moment of capture.
3. The image is imperfect due to lens distortions. Light passing through an imperfect lens will distort the

true representation of the physical area (Aber *et al.*, 2010).

In order to assess the variability in how accurately the applications interpret GSD compared to the theoretical GSD, an analysis was completed determining GSD at three points in the project workflow:

1. Using the above equation with the average elevation input based upon geo-tagged imagery information.
2. Using the above equation with elevation based upon the photogrammetry application's external orientation estimation.
3. Using the photogrammetry application's bundle adjusted output reported GSD (the cell size of the resulting orthomosaics).

Results

Camera Calibration

The results of the camera calibration are summarized here to compare results from the three camera calibration objects and the results from calibrations before and after flight. A detailed examination of the calibration results is beyond the scope of the research but is summarized to illustrate the discrete variations present between calibrations. The three parameters considered of highest importance were focal length, principle point, and radial distortion for two reasons. First, these are the characteristics typically required by photogrammetry software, and second, these parameters are subject to change by external and environmental forces such as shock, air pressure, temperature and humidity. This can lead to inconsistency in the photogrammetric process where interior camera orientation parameters are required.

Focal length of both cameras did show changes between calibrations (Figure 7). The Canon G10 was initially calibrated with a focal length of 6.3891 mm using the USGS cage. Its focal length was shown to vary on average by 9.367 μm in subsequent calibrations. The Canon S60 was initially calibrated with a focal length of 6.0271 mm using the USGS cage. Its focal length was shown to vary on average by 2.967 μm in subsequent calibrations, 6.4 μm less compared to the G10.

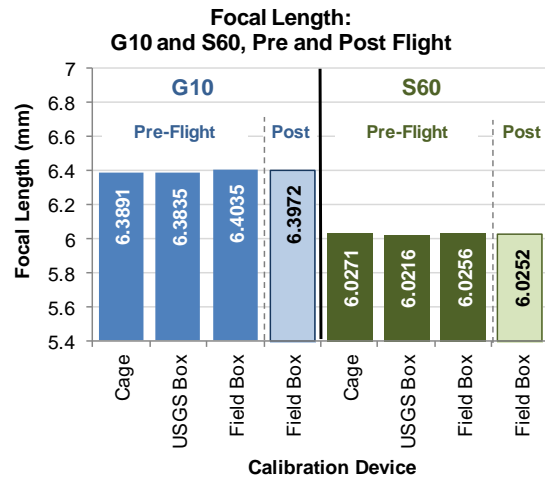


Figure 7. Focal length (mm) results from the camera calibration objects for the Canon G10 (blue) and Canon S60 (green) pre- and post-flight.

Radial distortion correction is the measure of how much each image would need to be corrected to remove the distortion calculated by the calibration procedure. It is therefore feasible to correlate the variances in correction values to movement of the internal lens elements. The radial distortion observed did show changes between calibrations (Figure 8). For the Canon G10 the greatest change from the USGS cage control calibration was observed in the USGS box calibration (20 μm at 4.5 mm radius). For the Canon S60 the greatest change from the USGS cage control calibration was observed in

the USGS box calibration (15 μm at 4.5 mm radius).

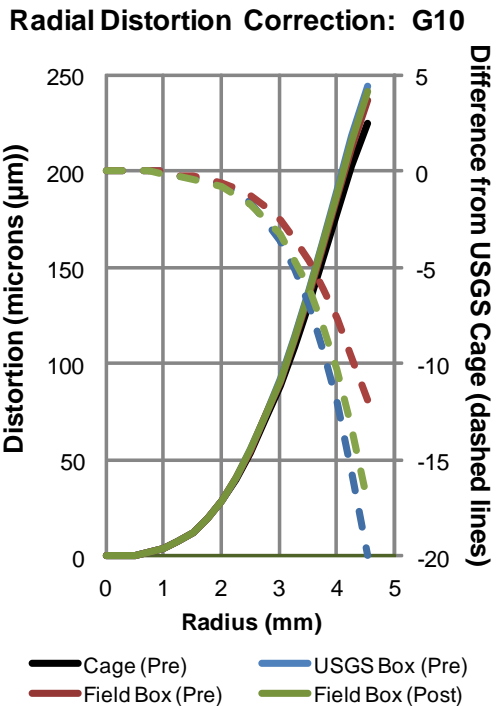
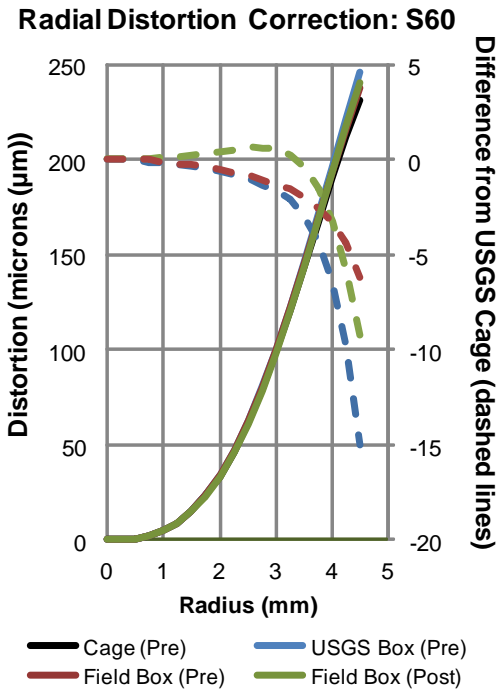


Figure 8. Radial Distortion (μm) analysis output from the camera calibration objects (solid lines) and difference from the USGS cage (μm ; dashed lines) for the Canon S60 (top) and Canon G10 (bottom).

The principal point, according to Eos Systems, Inc. (2010), is “the location in a camera where the optical axis of the lens intersects the imaging plane. It is the reference point in the image to which all marks and lens distortion parameters are related.”

In practice, the principal point will deviate off axis of center and is calculated as a correction in the camera calibration report. For each of the cameras it is shown that that the principal point was not stable and did shift in each calibration performed (Figure 9).

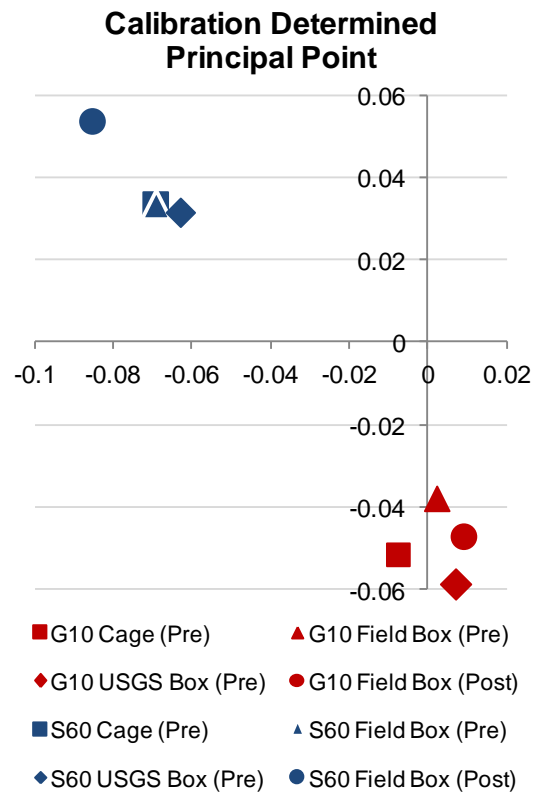


Figure 9. Principal Point calibration correction (mm) analysis. Change between calibrations is represented in xp, yp.

Functional Performance Measures

Ground Sample Distance Analysis

Each photogrammetry software reported a calculated GSD of the resulting

orthoimagery (Table 1). On average ERDAS produced the largest GSD at 2.33 cm per pixel, followed by Pix4D with 2.30 cm per pixel and Agisoft PhotoScan 1.92 cm per pixel using both camera datasets.

Table 1. Final ground sample distance (GSD) for imagery obtained by the Canon G10 and Canon S60 and processed with one of three photogrammetry software packages.

Software	Camera	GSD (cm/pixel)
ERDAS LPS	G10	1.82
	S60	2.3
Pix4D	G10	1.10
	S60	3.50
Agisoft PhotoScan	G10	1.21
	S60	2.63

The analysis comparing the two cameras shows the Canon G10 averaged a GSD of 1.3 cm per pixel. The Canon S60 showed an average GSD of 2.99 cm per pixel, a 130% increase over the Canon G10.

These post-processed GSD results were compared to the pre-processed theoretical GSD predictions calculated using the equation described in the methods (Figure 10). The theoretical GSD was calculated once using the average camera elevation based on image geotag information and again based on the camera’s external orientation determined by the software.

The results show the resulting GSD for both PhotoScan datasets were better than expected. This is likely to due GPS’s inherent lack of vertical precision causing error in initial elevation estimates which were later corrected by the software. The Pix4D Canon S60 GSD calculated using the software’s estimated external camera orientation show the most difference from predicted values. This appears to be due to an anomaly in how the software interpreted the geotagged

image elevation. However, the final resulting GSD values were within expected tolerances.

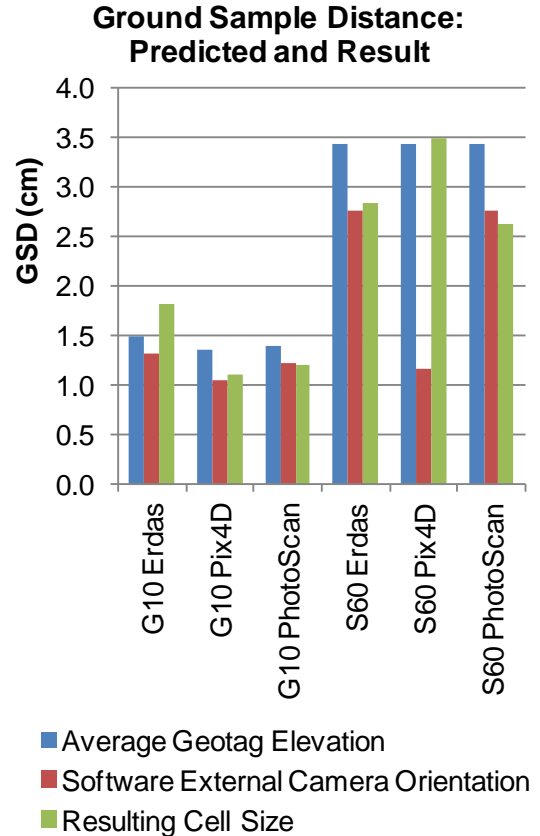


Figure 10. Ground sample distance (GSD) for imagery obtained by the Canon G10 and Canon S60: based on photo geotag elevation (blue), based on software determined external camera orientation information (red), and final cell size of orthoimagery (green).

Ground Control Point Accuracy Comparison

Ground control point accuracy was examined by comparing the RTK GPS control points locations against visual target locations for each orthomosaic. The distance was measured from the center of each aerial target to the corresponding ground control point. The differences in X and Y directions from the target center were documented (Figure 11).

Canon G10 imagery processed with Agisoft PhotoScan resulted in 2.14 cm average error and Canon S60 imagery processed with Agisoft PhotoScan had an average 2.10 cm error. The averaged error was 2.12 cm. Pix4D combined average error was 9.312 cm and ERDAS's average was shown to be 10.25 cm in error (Figure 12).

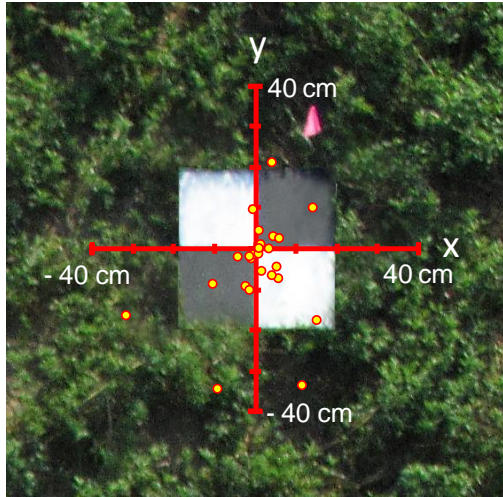


Figure 11. Scale GCP error representation of ERDAS processed G10 imagery in relation to a sample aerial target.

DTM Analysis

The examination of the digital terrain models resulted in an observed trend between smaller GSD and increased 3D surface area. Where the Agisoft PhotoScan Canon G10 dataset proved to have the highest 3D surface area of 10,477.52 ft², the ERDAS Canon S60 was shown to have the lowest 3D surface area of 9896.62 ft². This represents a 5.87% decrease in total surface area (Figure 13).

Pixel Classification

The image pixel classification analysis was implemented to calculate from within ArcMap the difference between the known total white area of the aerial targets versus

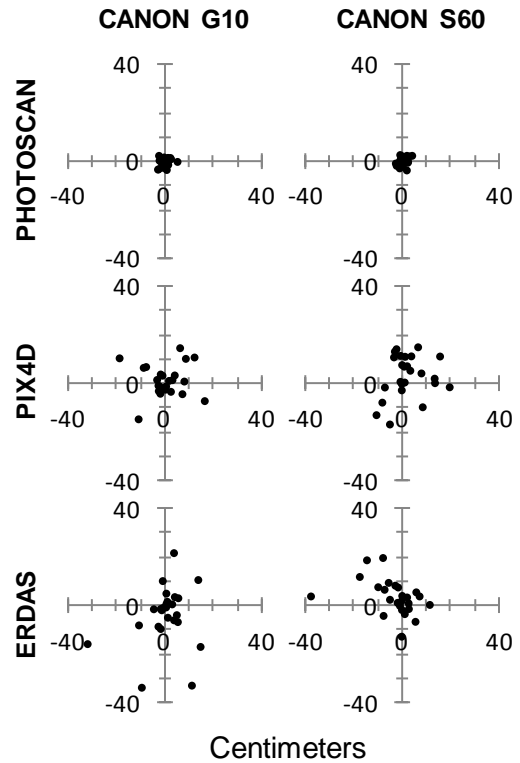


Figure 12. Ground control point (GCP) error index. The direct comparison between camera and application.

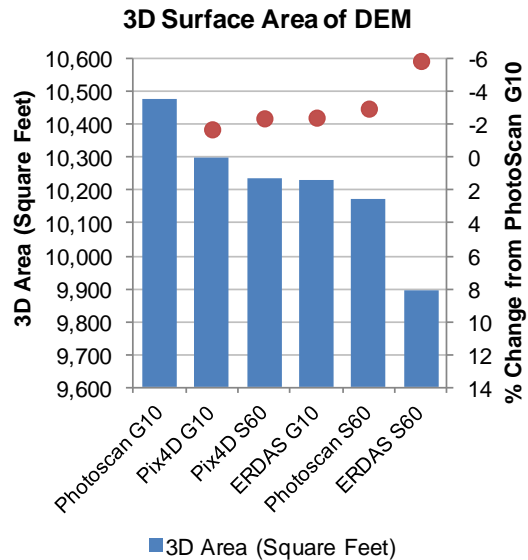


Figure 13. Difference in 3D surface area per application represented in square feet and percentage change from PhotoScan G10.

the orthoimage classified white area (Figure 14). Pix4D processed Canon S60 imagery represented a 9.04% increased area. The greatest difference was observed in Canon G10 Pix4D at a 13.477% increase. The results were inconclusive and will be discussed further below.

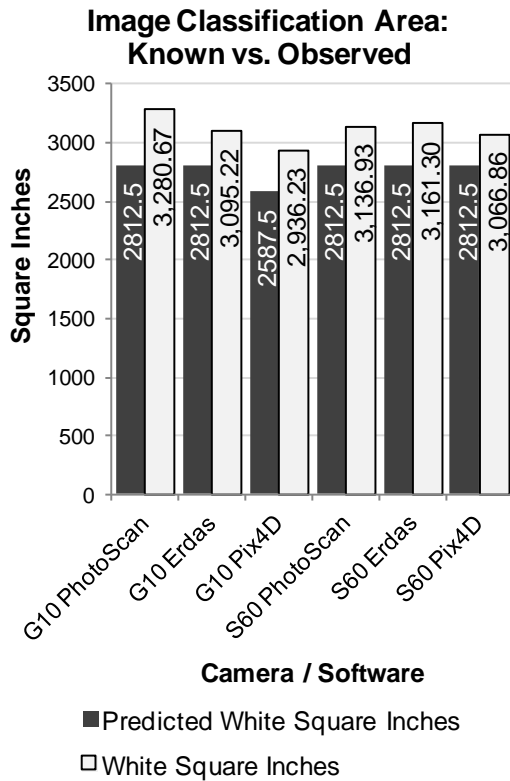


Figure 14. Image classification analysis. Known area of the white area of the aerial targets (black bars) compared to the resulting area found by image classification (light grey bars).

Discussion

Sources of Error

The probable sources of error in this research are mainly:

- 1) The altitude variability above the ground and overlap of images. Mosaicing and processing images from dramatically different altitudes and overlaps is not ideal. Images that are consistently of the

same overlap and elevation above ground would reduce error.

- 2) Variability in the environmental conditions between the flights. Atmospheric conditions such as turbulence, wind speed, humidity and available ambient light are notable variable factors between the data collection flights.
- 3) Lens and sensor variability between calibrations. Mechanical variability in the non-metric variable zoom camera lenses used in this research may introduce error. Variability may be caused by external shock or vibration upon the camera. Variation may be caused by relative temperature or humidity acting on the camera's materials. Variability may be a result of the combination of the aforementioned factors.
- 4) Human error. User interpretation of the aerial target image centers and the manual selection of ground control point entry for each software package could vary. Error could also exist during software project setup and in procedural fine-tuning.
- 5) Aircraft performance from flight to flight. Physical changes to the aircraft, center of gravity, equipment configuration or position could affect a change in how the aircraft would fly from one flight to the next.
- 6) Minimal sampling of datasets in both the camera calibrations and flights. Due to the window of opportunity to conduct the imaging research flights, only a limited number of flights were completed. To reduce sampling error more flights should be flown and more samples should be included.

Camera Calibration Stability

The camera calibrations have illustrated that there is variability in the lenses and that the calibrations are not consistent when compared across the range of cameras and calibration objects used in this research. When the pre and post field box calibrations for the Canon G10 and Canon S60 were compared, variability was still observed between calibrations, with the Canon G10 having a 5.2 μm difference in radial distortion at 4.5 mm and Canon S60 having a 3.2 μm difference in radial distortion at 4.5 mm. However, it appears that the variability observed in the calibrations may be compensated for in the post-processing of datasets.

Camera Performance

The Canon G10 camera was expected to produce higher resolution imagery over the Canon S60 strictly based on the Canon G10 higher theoretical sensor and lens capabilities. This correlation was observed in the GSD analysis where Canon G10 cm/pixel results were consistently of a higher resolution than the Canon S60. The GCP accuracy comparison analysis indicates that the Canon G10 and Canon S60 were virtually identical. Variances in the values were too small to draw a definite conclusion as to which camera performed better in this test. This could be affected due to where the image centers were interpreted.

The DTM analysis sought to compare the three dimensional area of the DTMs. The goal was to observe if a higher resolution DTM would affect the total three dimensional surface area and what, if any, relationship existed between the DTMs and GSDs. The PhotoScan Canon G10 dataset yielded the largest 3D surface area at 10477.52 ft^2 followed by the Pix4D

Canon G10 dataset at 10301.11 ft^2 . The third largest surface area dataset was the Pix4D Canon S60 dataset with a 3D area of 10233.88 ft^2 , narrowly exceeding the ERDAS Canon G10 with a 3D area of 10229.55 ft^2 by just 4.33 ft^2 . The results are somewhat surprising being that the Pix4D Canon S60 dataset had more surface area than the ERDAS Canon G10 even though the Pix4D Canon S60 dataset had a larger GSD than the ERDAS Canon G10.

Software Performance

ERDAS LPS, a traditional production level photogrammetry application for commercial and government wide-area imaging is vastly more robust and complex than the other two applications in the study. However, its routines and logarithms are generally specific in terms of what the application expects as input data. ERDAS LPS expects data to be generally from the same altitude and of near nadir at the time of capture. ERDAS LPS was designed to process imagery from manned piloted aerial aircraft and satellite imaging where altitude above the ground can be tightly controlled and reported. Furthermore, the pitch, roll, and yaw angles of the aircraft are more easily controlled by employing sophisticated gimbal systems that allow the imaging sensor to maintain near nadir position during data capture. Initial findings of this research appear to show that consistency in image overlap and altitude has a larger effect on the overall accuracy when the application workflow is expecting this type of imagery. The Canon G10 ERDAS imagery was taken from various elevations and off-nadir orientations throughout the flight (Figure 15), whereas the Canon S60 imagery was taken as a single series of images along one flight line (Figure 16).

The GSD results for the Canon G10 imagery processed with ERDAS LPS was natively better than the Canon S60 due to the sensor size; however, it was worse than the geotag elevations would have predicted. This difference is likely due to the software not anticipating images from dramatically different elevations and orientations off nadir.

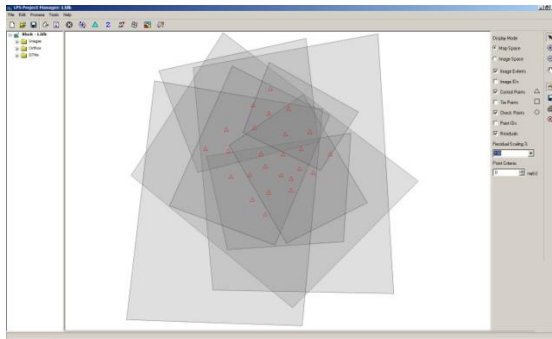


Figure 15. Screen capture of the ERDAS LPS interface illustrating the Canon G10 image footprints in the Block file. Note the variations in footprint size and orientation.

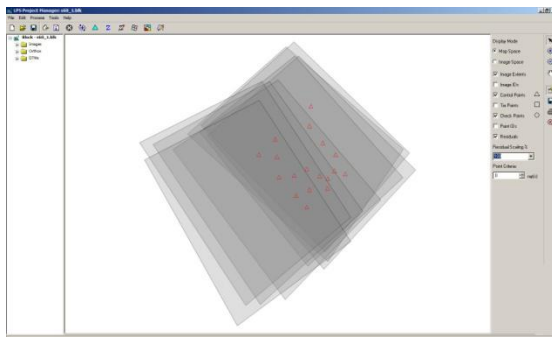


Figure 16. Screen capture of the ERDAS LPS interface illustrating the Canon S60 image footprints in the Block file. Note the consistency in footprint size and orientation.

Improvements in final GSD relative to predicted GSD were seen with both the Pix4D and PhotoScan applications, suggesting these programs by design are likely less sensitive to variation in image elevation than ERDAS LPS.

Whereas the applications ERDAS LPS and Agisoft PhotoScan accept interior orientation information input to obtain exterior camera orientation, Pix4D does

not require interior orientation information as an input, possibly affecting overall quality.

Image Performance

There was variability found in the analysis of the datasets processed in ArcMap. The image classification analysis sought to calculate within ArcMap the difference between the known total white area of the aerial targets vs. the observed classification area within the derived datasets. The results obtained from the image classification were not expected. A trend was expected between GSD and classification accuracy where more accurate classification results would be expected with smaller GSD. This trend was not observed possibly due to: 1) the phenomenon called image bloom where brighter areas of an image grow relative to their actual size, and 2) inaccurate classification parameters used in analysis. More work could be done in the future to refine the parameters or test alternative image classification scenarios.

Variability and consistency are the largest hurdles that need to be addressed when assessing the capabilities of UAV survey systems against commercial aerial imagery products. Considerations of how environmental and procedural variability can affect the datasets need to be addressed and if that variability is within acceptable tolerances for the project at hand. Additional sampling and testing needs to be conducted in order to develop a truly accurate measure of the variability observed in the research.

Future Research

Future research would seek to extend upon the initial findings of this research. First, to conclude that any specific unmanned

aerial survey vehicle can produce a dataset of certain quality, it is the author's assertion that claims of capability should be based upon dozens, if not multiple dozens of nearly identical data collection flights. Second, moving beyond multiple sensors and multiple image processing applications, one camera sensor and one image processing application should be chosen for the future research to provide consistency over the range of future flights. If there is any doubt regarding a particular application or sensor, the examination of other cameras and application combinations could be explored utilizing the above methodology of testing one sensor against one application.

Conclusion

The research has illustrated a process for comparing unmanned aerial survey datasets from two cameras and processed through three photogrammetry software applications. The analysis for the research was conducted solely from within the Esri GIS environment and was intended to identify and isolate the relationships between the cameras and software where possible. The research suggests the process and methodology is capable of producing high-resolution spatially accurate data that is comparable if not better than current commercial deliverables for small areas of study. With typical current commercial imagery provided at 15.24 cm GSD, this research was able to achieve 1.92 cm GSD.

Reliability and consistency of the cameras was analyzed from comparisons in the calibration. Reliability and consistency of the cameras was observed to be acceptable. The photogrammetry applications used in the research appear to expect some variation and are able to

compensate for that variable input and still produce reasonable results. Spatial accuracy was tested by comparing where the aerial targets centers resided in the images to the actual GCP coordinates. The overall spatial accuracy achieved in the research should be considered accurate enough to service small areas of research where aerial remote sensing is needed but would be otherwise be too cost-prohibitive and time-sensitive to fulfill with traditional commercial aerial datasets. Project findings support the value of continued research into unmanned aerial survey vehicles in conjunction with non-metric cameras to produce viable geospatially accurate datasets.

Acknowledgements

Special thanks to the following individuals and organizations that have contributed to this research:

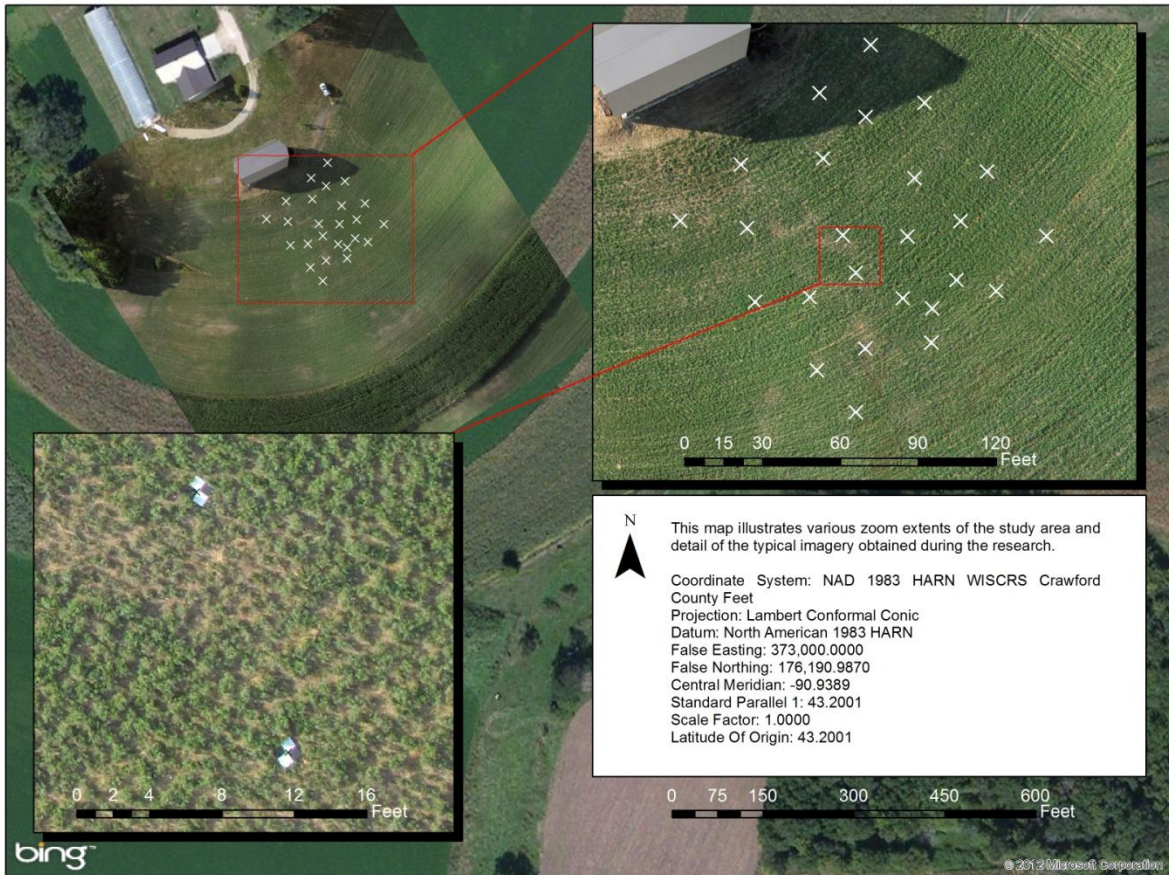
- Larry Hanson
- Al Slavick
- Joerg Feldbinder of Paragon Associates
- Don Moe of the USGS
- John Ebert of Saint Mary's University
- Dr. McConville of Saint Mary's University
- Greta Bernatz of Saint Mary's University
- Jerome Johnson of Winona State University Composite Materials Engineering program
- Don Ritzenthaler
- Al Poser
- Patricia Poser

References

Aber, J. S., Marzolff, I., and Ries, J. B. 2010. Small-Format Aerial Photography:

- Principles, Techniques and Geoscience Applications. Elsevier. Oxford, UK.
- Abramson, L. 2012. Drones Drifting Into Markets Outside War Zones. National Public Radio. Retrieved September 19, 2012 from <http://www.npr.org/2012/08/13/158715809/drones-drifting-into-markets-outside-war-zones>.
- Agisoft. 2012. Agisoft PhotoScan – Capabilities. Retrieved September 19, 2012 from <http://www.agisoft.ru/wiki/PhotoScan/Capabilities>.
- American Society of Photogrammetry and Remote Sensing (ASPRS). 2009. Guidelines for Procurement of Professional Aerial Imagery, Photogrammetry, Lidar and Related Remote Sensor-based Geospatial Mapping Services. Retrieved September 3, 2012 from http://www.asprs.org/a/society/committees/standards/Procurement_Guidelines_w_accompanying_material.pdf.
- BAE Systems. 2010. Glossary of Terms. Retrieved from http://www.socetgxp.com/docs/support/socet-gxp_glossary-of-terms.pdf.
- Canon. 2012a. About PowerShot G10. Retrieved September 2, 2012 from http://www.usa.canon.com/cusa/support/consumer/digital_cameras/powershot_g_series/powershot_g10#Specifications.
- Canon. 2012b. About PowerShot S60. Retrieved September 2, 2012 from http://www.usa.canon.com/cusa/support/consumer/digital_cameras/powershot_s_series/powershot_s60#Specifications.
- Eos Systems, Inc. 2010 Glossary. Retrieved November 29, 2012 from <http://www.photomodeler.com/support/glossary.htm>.
- ERDAS. 2010. ERDAS Field Guide. ERDAS, Inc. Norcross, GA.
- Matthews, N. A. 2008. Aerial and Close-Range Photogrammetric Technology: Providing Resource Documentation, Interpretation, and Preservation. Technical Note 428. U.S. Department of the Interior, Bureau of Land Management, National Operations Center, Denver, Colorado. 42 pp. Retrieved September 25, 2012 from <http://www.blm.gov/nstc/library/pdf/TN428.pdf>.
- Professional Aerial Photographers Association. 2012. History of Aerial Photography. Retrieved September 3, 2012 from <http://www.papainternational.org/history.asp>.
- Stahlke, E. 2011. Aerial Perspective: Close-range Aerial Photogrammetry Comes of Age. Professional Surveyor Magazine. Retrieved September 2, 2012 from <http://www.profsurv.com/magazine/article.aspx?i=70968>.

Appendix A. Project Imagery of Study Area.



The ArcMap layout above illustrates the research imagery's orthomosaic spatial orientation and scale in relation to Microsoft's Bing Map base layer.